A Cryogenic System With High Capacity and Efficiency for HTS Cable

Renjun Xue, Jun Tan, Yongjiang Zhao, Bangjian Zhao, Han Tan, Yujia Zhai, Shiguang Wu, Dong Ma, Dirui Wu, and Haizheng Dang

(Invited Paper)

***Abstract*—For mega-cities with growing electricity demands, the High-Tc superconducting (HTS) cables, owing to the distinct advantages of high electrical capacity and current density, become promising solutions to power grid reconstruction and expansion. The cryogenic system is expected to provide a vital low-temperature environment to ensure the steady operation of the superconductors. A cryogenic system based on the high-capacity Stirling-type pulse tube cryocooler (SPTC) developed in the authors' laboratory is now under coupling test with a short test line of the HTS cable. The aim is to meet stringent requirements such as high reliability, low maintenance, and high refrigeration efficiency which are desirable for the cables. The cooling capability of the SPTC in the HTS cable cryogenic system reaches 950 W at 72 K with a high relative Carnot efficiency (RCE) of about 14.5 % during the onsite coupling test with the HTS cable system. This paper will present the overall composition, operation mechanism, and integration technology of the cryogenic system for the HTS power cable in detail. The SPTC has been custom-developed for convenient and demountable connection with the cryogenic lines. The flow circulation, reliability design, and thermal analysis are also introduced. The performance characteristics and testing results will be presented and discussed as well.**

***Index Terms*—Cryogenic system, stirling-type pulse tube cryocooler, high-Tc superconducting cable, integration technology, feasibility verification.**

Manuscript received 26 September 2023; revised 27 November 2023; accepted 27 November 2023. Date of publication 1 December 2023; date of current version 12 December 2023. This work was supported in part by the National Natural Science Foundation of China under Grant 52076210, in part by the Major Project of Science and Technology Commission of Shanghai Municipality under Grant 22511100100, in part by Shanghai Municipal Science and Technology Major Project under Grant 2019SHZDZX01, in part by the Collaborative Innovation Project of Shanghai Municipality under Grant XTCX-KJ-2023-58, and in part by Shanghai Municipality under Grant 20ZR1466100. *(Corresponding authors: Renjun Xue; Haizheng Dang.)*

Renjun Xue, Jun Tan, Yongjiang Zhao, Bangjian Zhao, Han Tan, Yujia Zhai, Shiguang Wu, Dong Ma, and Dirui Wu are with the State Key Laboratory of Infrared Physics, Shanghai Institute of Technical Physics, Chinese Academy of Sciences, Shanghai 20083, China, and also with the University of Chinese Academy of Sciences, Beijing 100049, China (e-mail: cryoxrj@163.com; juntan@mail.sitp.ac.cn; yjzhao13@163.com; zhaobjq@163.com; hantancryo@163.com; cryozyj@163.com; 1071264083@qq.com; madongsdu@126.com; 1132996314@qq.com).

Haizheng Dang is with the State Key Laboratory of Infrared Physics, Shanghai Institute of Technical Physics, Chinese Academy of Sciences, Shanghai 20083, China, and with the Shanghai Research Center for Quantum Sciences, Shanghai 201315, China, and with the University of Chinese Academy of Sciences, Beijing 100049, China, and also with the Shanghai Boreas Cryogenics Company Ltd., Shanghai 201802, China (e-mail: haizheng.dang@mail.sitp.ac.cn).

Color versions of one or more figures in this article are available at https://doi.org/10.1109/TASC.2023.3338133.

Digital Object Identifier 10.1109/TASC.2023.3338133

I. Introduction

WITH the continuous growth of the city, the electricity demand in the downtown area is also increasing. For the mega-cities around the world, HTS cable applications owe the superiorities of large electrical capacity, high current density, and small space occupation, and thus become more preferred solutions for urban power grid reconstruction and power capacity expansion [1]. Meanwhile, HTS power cables are regarded as revolutionary technologies in power transmission due to their remarkable features, including zero electromagnetic radiation, magnetic immunity, compact structure, low power loss, and energy conservation [2], [3], [4], [5].

To provide the appropriate low-temperature working environment for HTS devices, the cryogenic system is one of the vital supporting facilities to ensure the steady operation of the cables. As an essential component in the HTS cable system, the compactness, efficiency, and reliability of the cryogenic system are the key concerns for the practical application. For the HTS power cable, the used material and manufacturing technology itself is relatively mature. However, the problems associated with the used cryocoolers have hampered the advance of their future widespread applications to some extent.

Low maintenance, high reliability, long operation life, high cooling efficiency, compact size, and acceptable cost are the typical requirements for the cryocoolers used in the HTS system. At present, cryocoolers used in the HTS cable cryogenic systems mainly include Stirling, GM, reverse Brayton, and pulse tube cryocoolers [6], [7], [8], [9]. Among these, the reverse Brayton cryocooler is the least commonly used due to its complex structure, low efficiency, and high noise levels. Stirling cryocoolers with crank-link mechanisms and GM cryocoolers with displacers and adsorbers all need regular maintenance, typically scheduled every 6000 to 10000 hours. The pulse tube cryocooler without any moving component in the cold head has the intrinsic merits of a long lifetime, and the Stirling-type pulse tube cryocooler (SPTC) driven by the linear compressor achieves high reliability from the driving source.

A cryogenic system for cooling the HTS cable based on the SPTC has been designed and built and is now under the coupling test with superconducting cable. The used SPTC is inherited from a series of ones developed for aerospace applications in the authors' laboratory and thus keeps the merits of reliable performance and long service life which is expected to reach 50000 hours [10], [11], [12]. With outstanding features achieved during the laboratory experimental tests [13], such as a high cooling capacity reaching 1220 W at 77 K with the corresponding relative Carnot efficiency (RCE) of 16.7 % and a wide cooling temperature varying from 45 K to the ambient temperature, the SPTC is regarded as an attractive cryocooler for the HTS cable applications. As a result, further application validations are carried out in the HTS cable system to evaluate the SPTC's practical performance.

In this paper, the overall design, operation mechanism, coupling structure, and integration technology of the cryogenic system with the SPTC for the HTS power cable will be described. The flow circulation, reliability design, and thermal analysis are also introduced. The performance characteristics and results of the developed cryogenic system in the onsite tests will be presented and discussed as well.

II. HTS Cable System Integrated With the SPTC

A. Design of the Cryogenic Circulation System for HTS Cable

In this study, the cold dielectric HTS cable manufactured with the second-generation YBCO wire is the core component cooled in the superconducting cryogenic system.

As shown in Fig. 1, the cryogenic system employs a hybrid configuration combining close-looped and open-looped refrigeration with the aim of enhancing reliability. The close-looped system primarily consists of the superconducting cable, LN_2 pump, subcooled LN_2 storage tank, filter, buffer tank, and cryocooler unit with heat exchangers. Simultaneously, a vaporizer and a vacuum pump are connected to the subcooled LN_2 storage tank, working as the main components of the open-looped refrigeration part. The open-looped system can immediately activate to maintain the temperature in the cryogenic system by depressurization and venting when the close-looped refrigeration fails to work properly, preventing the loss of superconductivity due to a rapid temperature increase.

B. LN_2 Circulation and Operation Mechanism

The LN_2 circulation works in the closed-loop system integrated with the SPTC. Within the circulation, nitrogen, the working fluid, is subcooled to the LN_2 temperature by the heat exchanger fixed at the cold end of the SPTC. Once cooled by the cryocooler, the sub-cooled LN_2 will accumulate in the storage tank. Then driven by the pump unit, it flows into the cooling channel inside the HTS cable to counteract heat losses and maintain the cable's working temperature below 77 K. Subsequently, the LN_2 flows through a filter to remove small solid impurities and enters the buffer tank before returning to the cryocooler unit for recooling in the next circulation.

Fig. 2 depicts the design for the HTS power cable part in the cryogenic system. During normal operation, the subcooled LN_2 flows through the HTS cable to maintain its superconducting state for low-loss and high-efficiency power transmission. Sensors and valves are positioned both at the cable's inlet and outlet, as well as inside the cable itself. One control valve is employed at

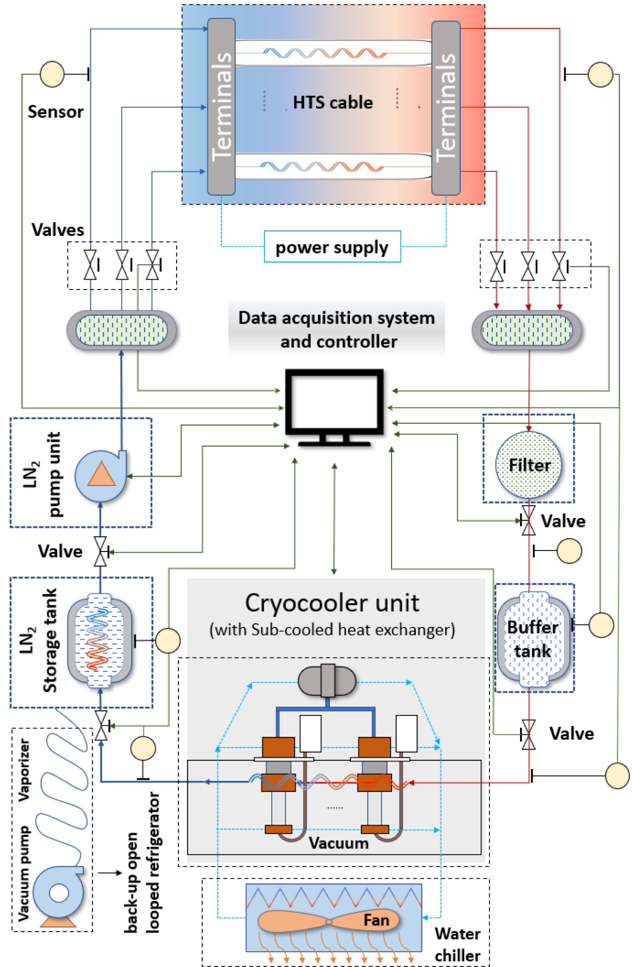

Fig. 1. Configuration and operation process of the cryogenic system based on the SPTC for the HTS cable application.

the inlet to adjust the mass flow rate into the cable based on the data from the sensors. Additionally, another auto-relief valve is positioned at the outlet for safety purposes, preventing the pressure in the pipelines from exceeding the maximum allowable working pressure.

C. Coupling Structure of the SPTC and Control Solution

In this designed cryogenic system for HTS cable cooling, the developed SPTC employs the inline cold finger driven by the dual-opposed linear compressor. The cold finger is mainly composed of the aftercooler, regenerator, cold-end heat exchanger, pulse tube, and warm-end heat exchanger. The inertance tube with the reservoir is the only phase shifter in the cryocooler. A typical cooling capacity of 1220 W at 77 K is achieved under an input power of 20 kW by applying one linear compressor to drive two cold fingers in our previous experimental research [13]. In order to meet the requirements of practical applications, the SPTC has been specially designed to interface with the cryogenic system for the HTS cable.

1) Coupling Structure Between the SPTC and the LN_2 Lines: As depicted in Fig. 3, the cryocooler has been custom-designed

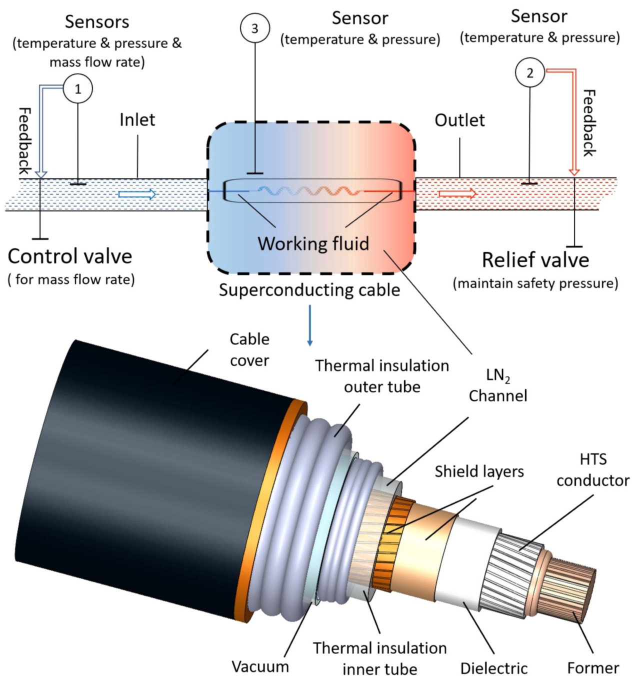

Fig. 2. Schematic of the HTS cable part.

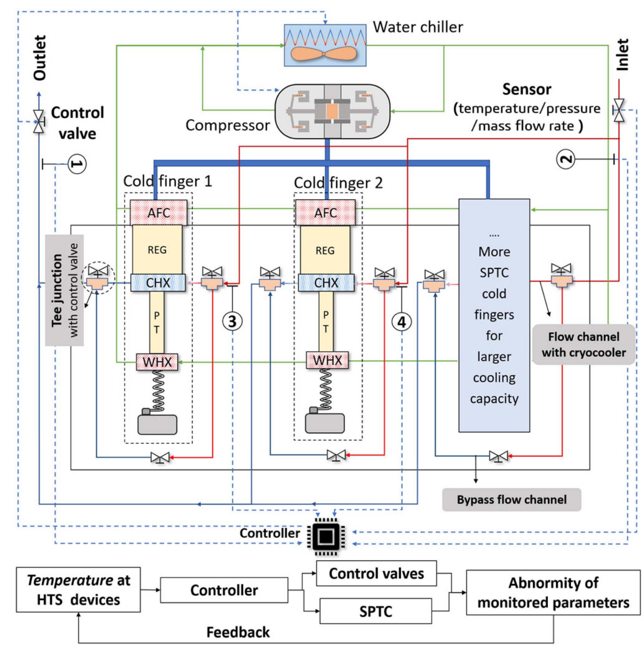

Fig. 4. Reliability design and control mechanism for the cryocooler unit.

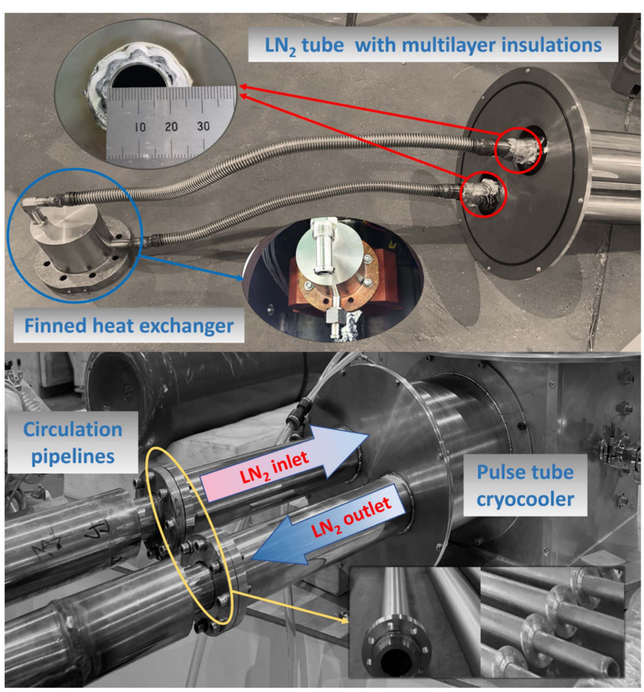

Fig. 3. Schematic of the coupling structure between the cryocooler unit and the LN_2 circulation pipeline.

for convenient integration with the LN_2 circulation pipelines. For the inlet and outlet of LN_2 pipelines connected with the cryocooler's cold head vacuum chamber, vacuum-insulated pipes with Bayonets and flange connections have been used. The cryogenic parts employ *Teflon* liquid seals, while *Kel-F* O-ring gas seals are utilized in the ambient-temperature part. This standardized interface facilitates the demountable piping joints, realizing the quick connections between the LN_2 pipelines with the SPTC.

In terms of heat transfer, the finned-type heat exchanger is employed and fixed on the surface of the cold-end surface in the SPTC. Heat conduction is the main way for cooling the heat exchanger by the cryocooler. Liquid nitrogen is further cooled by the heat exchanger to its subcooled state and accumulates before flowing out.

During the installation and integration, it should be noticed that the LN_2 lines need to be wrapped with multi-layer insulations to minimize heat loss. In the designed system, aluminized polyester film and fibrous layer are used.

2) Solution and Flow Control System to Improve Reliability: Fig. 4 demonstrates the reliability design and control mechanism for the cryocooler unit. As vividly shown, each cold finger operates independently, and multiple ones can be integrated to produce a larger cooling capacity.

Additionally, a bypass pipeline is installed at each cold head. If one cold finger in the cryocooler unit fails to work normally or breaks down, the controller will redirect the LN_2 flow into the bypass flow channel by adjusting the control valves located at the Tee junctions. This reliability solution ensures that the other cold fingers can continue to operate normally in the above-mentioned circumstances, preventing a rapid temperature increase in the system and enhancing stability and reliability.

Furthermore, the controller can monitor temperatures at the key positions in the cryogenic system and adjust the input power of the SPTC linear compressor accordingly. This allows for flexible adjustments of the cryocoolers' cooling capacity, reducing power consumption when the thermal load decreases.

D. Factors Causing the Loss in the System

When designing the cryogenic system, several key factors causing the loss in flow and heat transfer need to be considered.

1) Flow Resistance: The flow resistance is reflected by the pressure drop along the tube. The pressure drop along the flow direction can be evaluated by the equation below:

$$\Delta P = f \cdot (l/d) \cdot (\rho \cdot v^2) / (2g) \quad (1)$$

where ΔP represents the pressure drop along the flow direction, f is the friction loss factor which can be calculated with the Reynolds Number, l and d are the length and diameter of the tube, ρ represents the density, and g is the gravitational acceleration.

2) Heat Leakage of the Vacuum Transfer Pipe: The heat leakage of the vacuum transfer pipe brings extra heat load to the cryogenic system The transfer lines cannot be exposed to the air directly. The multilayer insulation materials and the vacuum insulated pipelines are employed to reduce the heat leakage including the radiation heat transfer loss and convective heat transfer loss of the transportation pipes.

The heat leakage of the pipe includes the heat leakage Q_1 of the multilayer insulation materials and Q_2 of the supporting component inside the pipe. The Q_1 can be calculated by [14]:

$$Q_1 = K \cdot F_m \cdot (T_2 - T_1) / \delta \quad (2)$$

where K is the apparent thermal conductivity of multilayered materials, T_1 is the inner wall temperature, T_2 is the outer wall temperature, F_m is the equivalent surface area, and δ is the thickness of the insulation material.

The heat leakage of the support is mainly due to the heat conduction, and it can be calculated by:

$$Q_2 = \lambda \cdot \Delta T \cdot A/L \quad (3)$$

where λ is the conductivity, A is the heat exchange area, and L is the thickness of the support.

3) Heat Leakage by the Cryostat of the Cryocooler Unit: The heat leakage of the cryostat is mainly caused by the radiation heat transfer loss between the internal surface of the vacuum chamber and the outer surface area of the cold finger and the pipelines, and can be calculated by [15]:

$$Q_D = \varepsilon_{1-2} \cdot \sigma \cdot F_1 \cdot \left(T_2^4 - T_1^4\right) \cdot \psi_{1-2} \quad (4)$$

where F_1 is the surface area of the cryocooler and pipeline, σ is the Stefan-Boltzmann constant, $\varepsilon_{1\text{-}2}$ and $\psi_{1\text{-}2}$ are the emissivity and view factor between the two objects.

4) Efficiency of the Heat Exchanger and the Cryocooler: Moreover, the actual efficiency of the heat exchanger and the SPTC operating in the cryogenic system can lead to a reduction in cooling performance compared with the theoretical value. The key factors influencing the efficiency of the heat exchanger are the equivalent heat exchange area, mass flow rate, and resistance of the working fluid. In terms of the developed SPTC, two significant efficiencies determine the actual cooling capability. The first is the compressor's efficiency, which represents the conversion rate from the input electrical power to the PV power. The second is the coefficient of performance (COP), which reflects the conversion rate from the PV power to the cooling power.

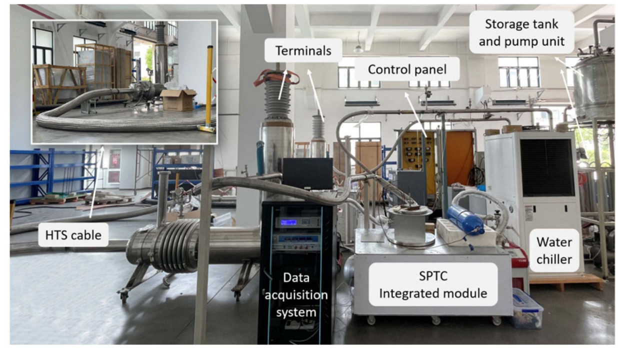

Fig. 5. HTS cable testing system integrated with the SPTC.

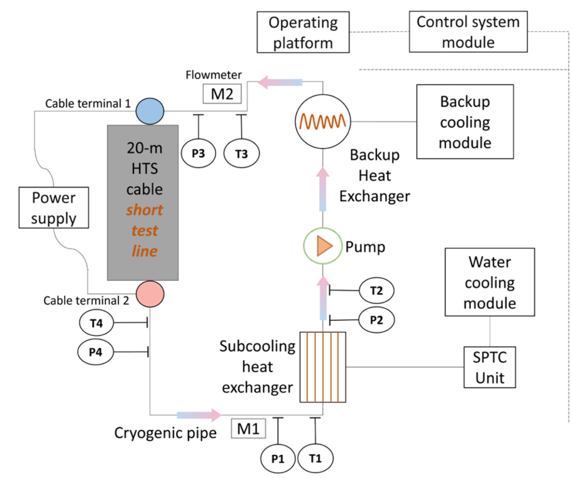

Fig. 6. Configuration of the test and setup for the sensors.

III. Performance Characteristics in the Test

A. Configuration and Setup for the Coupling Experiment

In order to investigate the actual cooling performance of the SPTC, the testing cryogenic system with the HTS cable short line, as shown in Fig. 5, was established to evaluate the feasibility and stability of the designed cryocooler when cooling the superconducting device.

The testing system is designed and built based on the employed SPTC with a cooling capacity of 1220 W at 77 K. Calculated cooling power consumptions are approximately 60 W for a 20-meter-long HTS cable, 600 W for two sets of terminations, 100 W for one joint box, and 200 W for the integrated low-temperature pipelines and other cryogenic components. A safety margin of 20 % is considered when calculating the theoretical total demand for the cooling capacity of 1152 W, which is within the SPTC's cooling capacity.

As shown in Fig. 6, sensors of temperature, pressure, and flow rate are installed at both ends for the cryocooler unit and HTS cable side. The experimental setups allow for real-time monitoring and data acquisition for calculating the cryocooler's

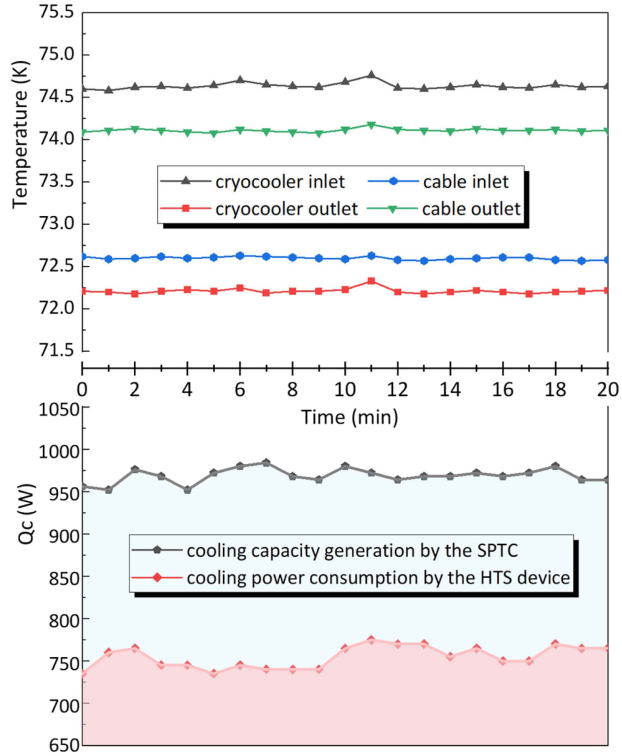

Fig. 7. Temperature curves and corresponding cooling power generation and consumption during the 20-minute operation of the cryogenic system.

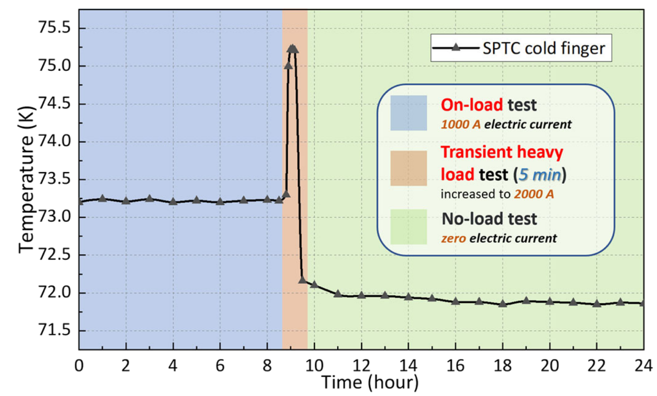

Fig. 8. Cooling temperature at the cold end of the SPTC in the 24-hour test with three typical working conditions.

cooling capacity and the cooling power consumption of the superconducting equipment.

The calculation for the cooling capacity and power consumption is based on the specific heat equation below:

$$Q_c = m \times C_p(T_{\text{in}} - T_{\text{out}}) \tag{5}$$

where T_{in} and T_{out} are the inlet and outlet temperatures of the cryocooler unit, C_p is the average specific heat of liquid nitrogen at constant pressure in the process, and m is the mass flow rate of the LN_2.

In the testing system, the charging pressure of the LN_2 is 8 bar. The designed temperature difference at both ends of the cable terminations is required within 2 K. The initial parameters of the used SPTC are as follows: The working fluid is the high-purity helium of 99.999 %. The charging pressure is 3.4 Mpa. The working frequency is 51 Hz. The temperature setting for the water chiller is 15°C.

B. Discussions on the Testing Results

Fig. 7 shows the temperature curves and the corresponding cooling powers produced by the SPTC and consumed by the HTS device during the 20-minute operation of the cryogenic system.

It can be seen that the temperatures kept relatively stable during the test. The highest temperature at the superconducting device part was below 75 K, which guaranteed the stable and normal operation of the HTS cable. The highest and lowest temperatures were recorded at the inlet and outlet of the SPTC, respectively. From the calculation results, the SPTC could provide an effective cooling capacity of more than 950 W for cooling the LN_2 flow when the cooling temperature was set to 72 K. Under this working condition, the SPTC achieved a high RCE of 14.5% with an input electrical power of 19.6 kW. The HTS cable devices consumed approximately 750 W of cooling power in the practical testing.

To further assess the reliability of the SPTC's cooling performance, a 24-hour long operation test has been conducted. Fig. 8 depicts the cooling temperature at the cold end of the SPTC cold finger in the longtime test with three typical operating conditions. Firstly, an on-load test with 1000 A electric current for 8 hours is performed, and the cooling temperature of SPTC is around 73.2 K. Then, the transient heavy load of 1000 A for 5 minutes is applied to the cable system. The cooling temperature was observably increased to 75.2 K. After that, the electric current was reduced to 0 A, which meant no load was applied to the HTS cable. During this period of the no-load test, the cooling temperature of the cold finger gradually decreased to 71.8 K and finally achieved stability. In all, the developed SPTC together with the HTS cable devices operated steadily and without any malfunction throughout the reliability tests.

IV. Conclusion

This article presents the design approach, integration technology, and coupling test of a cryogenic system employing the SPTC developed in the authors' laboratory for cooling the HTS cable. The composition and operation process of the cryogenic system coupled with the HTS cable are described and analyzed in detail. The demountable connection and the heat transfer mechanism between the cryocooler and the LN_2 circulation pipelines are introduced. The reliability design and flow control method for the engineering application are illustrated. The factors causing the loss in the system are summarized. Based on the results from the onsite test of the cryogenic system, the SPTC performed stably and could provide a cooling capacity of 950 W at 72 K with a high RCE of 14.5%. In conclusion, the tested HTS cable system operated in good conditions without any failure when cooled down by the SPTC unit. The above results indicate that the developed SPTC is a promising cryogenic system candidate for the future applications of the HTS cable.

REFERENCES

[1] A. Paramane, M. Awais, T. Chandrasekaran, M. Junaid, M. T. Nazir, and X. Chen, "A review on insulation and dielectrics for high- temperature superconducting cables for power distribution: Progress, challenges, and prospects," *IEEE Trans. Appl. Supercond.*, vol. 33, no. 6, Sep. 2023, Art. no. 4801831, doi: 10.1109/TASC.2023.3267055.

[2] B. G. Marchionini, Y. Yamada, L. Martini, and H. Ohsaki, "High-temperature superconductivity: A roadmap for electric power sector applications, 2015–2030," *IEEE Trans. Appl. Supercond.*, vol. 27, no. 4, Jun. 2017, Art. no. 0500907, doi: 10.1109/TASC.2017.2671680.

[3] X.-Y. Xiao, Y. Liu, J.-X. Jin, C.-S. Li, and F.-W. Xu, "HTS applied to power system: Benefits and potential analysis for energy conservation and emission reduction," *IEEE Trans. Appl. Supercond.*, vol. 26, no. 7, Oct. 2016, Art. no. 5403309, doi: 10.1109/TASC.2016.2594800.

[4] J. X. Jin et al., "Enabling high-temperature superconducting technologies toward practical applications," *IEEE Trans. Appl. Supercond.*, vol. 24, no. 5, Oct. 2014, Art. no. 5400712, doi: 10.1109/TASC.2014.2346496.

[5] X. H. Zong, D. Wei, Y. W. Han, T. Tang, Z. Y. Zhang, and Z. G. Yu, "Development of 35kV 2000A CD HTS cable demonstration project," in *Proc. IEEE Int. Conf. Appl. Supercond. Electromagn. Devices*, 2015, pp. 593–595, doi: 10.1109/ASEMD.2015.7453717.

[6] J. A. Demko et al., "Triaxial HTS cable for the AEP Bixby project," *IEEE Trans. Appl. Supercond.*, vol. 17, no. 2, pp. 2047–2050, Jun. 2007, doi: 10.1109/TASC.2007.897842.

[7] J. H. Lim et al., "Cryogenic system for 80-kV DC HTS cable in the KEPCO power grid," *IEEE Trans. Appl. Supercond.*, vol. 25, no. 3, Jun. 2015, Art. no. 5402804, doi: 10.1109/TASC.2014.2387393.

[8] S. Iwai et al., "A conduction-cooled REBCO magnet with a single-stage GM cryocooler and a stainless steel case for storing the coil and covering it from thermal radiation," *IEEE Trans. Appl. Supercond.*, vol. 27, no. 4, Jun. 2017, Art. no. 4603605, doi: 10.1109/TASC.2017.2674959.

[9] P. C. Michael, L. Bromberg, A. J. Dietz, K. J. Cragin, and C. Gold, "Design and test of a prototype 20 kA HTS DC power transmission cable," *IEEE Trans. Appl. Supercond.*, vol. 25, no. 3, Jun. 2015, Art. no. 5401005, doi: 10.1109/TASC.2014.2373824.

[10] H. Z. Dang et al., "Review of recent advances in Stirling-type pulse tube cryocoolers," *Inst. Phys. Conf. Ser.: Mater. Sci. Eng.*, vol. 502, no. 1, 2019, Art. no. 012034.

[11] H. Z. Dang, "Development of high performance moving-coil linear compressors for space Stirling-type pulse tube cryocoolers," *Cryogenics*, vol. 68, pp. 1–18, Feb. 2015.

[12] R. Xue et al., "A long-life, high-capacity and high-efficiency cryogenic system developed for High-Tc superconducting magnet applications," *IEEE Trans. Appl. Supercond.*, vol. 32, no. 6, Sep. 2022, Art. no. 4601405, doi: 10.1109/TASC.2022.3153234.

[13] R. J. Xue et al., "Thermodynamic characteristics of a single-stage stirling-type pulse tube cryocooler capable of 1220 W at 77 K with two cold fingers driven by one linear compressor," *Energy*, vol. 278, Sep. 2023, Art. no. 127968, doi: 10.1016/j.energy.2023.127968.

[14] M. Matusiak, "Investigation of the thermal insulation properties of multilayer textiles," *Fibres Textiles Eastern Europe*, vol. 14, no. 5, pp. 98–102, 2006.

[15] H. D. Baehr and K. Stephan, "Thermal radiation," in *Heat and Mass Transfer*. Berlin, Germany: Springer, 2011, pp. 612–664.